20th Australasian Fluid Mechanics Conference
Perth, Australia
5-8 December 2016

Blade Element Momentum Theory Extended to Model Low Reynolds Number Propeller Performance

R. MacNeill[1] **and D. Verstraete**[1]

[1]School of Aerospace, Mechanical and Mechatronic Engineering
The University of Sydney, Sydney, New South Wales 2006, Australia

Abstract

At low advance ratios, large sections of UAV propeller blades are stalled, and the Reynolds number faced by each blade can be low. Both conditions lead to difficulties in modelling propeller performance. The aerodynamic models coupled with blade element methods usually only provide aerodynamic data for an assumed airfoil section, between the stall angles and for a single Reynolds number, leading to breakdowns in modelling accuracy at low advance ratios. Additionally, rotational effects are often ignored when formulating blade element methods. In this paper, three dimensional scanning is used to accurately obtain the airfoil sections that make up a propeller blade. An aerodynamic database is formed for each airfoil section, across a wide range of angles of attack and Reynolds numbers. These databases are then modified to include the effects of rotation. The predicted performance of a number of propellers is then compared to wind tunnel test data. Significant improvement is shown relative to a generic blade element-momentum model, in particular when modelling the performance of smaller propellers.

Introduction

In recent years, an increased focus has been placed on unmanned aerial vehicles (UAVs). Propellers are the predominant propulsion type used for UAVs, especially for smaller unmanned systems [1]. The efficiency of the powertrain and propeller is the key component in the operating range of the vehicle. A great deal of research is therefore focused on more efficient powertrain technology for small UAVs [2–4], however the propellers used by most UAV platforms have a fixed pitch [1, 5]. For a fixed pitch propeller, optimal efficiency occurs for only one advance ratio, meaning UAV propellers will often be operating away from the optimal design point, especially at low advance ratios.

Blade element methods are widely used to model propeller aerodynamics due to their simplicity, efficiency, and relatively good accuracy. However at low advance ratios, where propeller sections are stalled and face low Reynolds number airflow, this accuracy begins to degrade as the aerodynamic models coupled with blade element methods are usually simplistic [6, 7]. Aerodynamic data is often only provided for an assumed airfoil section between the stall angles and for a single (typically high) Reynolds number. The lack of aerodynamic data for both high angles of attack and varying Reynolds number leads to difficulty in accurately modelling low advance ratio performance with blade element methods [6, 8–11].

To ensure the applicability of the aerodynamic lookup tables provided to the blade element method, the airfoil sections that make up the propeller blade must be known. It has been shown that using 3D scanning to capture the exact airfoil sections can lead to good agreement with experimental data [17, 23].

A number of models have been developed to synthesise high angle of attack aerodynamic data, using wind tunnel test data [12, 13], flat plate theory [14] and semi-empirical methods [15, 16]. Meanwhile, recent efforts have been made to account for Reynolds number effects with blade element methods [7,17,18].

First investigated by Himmelskamp [19], rotation is seen to significantly affect the aerodynamic coefficients of airfoil sections, in particular around stall. Efforts have been made to understand and predict these rotational effects [8,16,20–22], though the implementation of such effects to blade element methods has been rare [6–8, 15, 16, 18].

This paper intends to quantify the possible accuracy when modelling small propeller performance with a blade element-momentum method. Detailed methodology of the BEMT method can be found in the work by Phillips [24]. The accuracy improvements are made possible through modification of the aerodynamic database. The originality of the paper is derived from the combination of 3D scanning of a propeller blade with the application of rotational effects, the extension of aerodynamic data to high angles of attack, and the variation of aerodynamic data with Reynolds number, all of which have not been combined previously.

Methodology

To extract the exact airfoil sections that comprise the propeller blade geometry, each tested propeller was scanned using a David-3D^{TM} SLS-2 3D scanner. This process generates a high fidelity image of the complete blade geometry, as shown in Fig. 1a. This allows accurate measurements to be made of the propeller pitch, chord, and sectional aerodynamic shape at any radial position. Aerodynamic data can then be found for each of the relevant airfoils. This is in contrast to relying on manufacturer specifications or estimation as is often the case for relatively low fidelity propeller analysis. As seen in Fig. 1b, the airfoil shape changes significantly as a function of the blade radius.

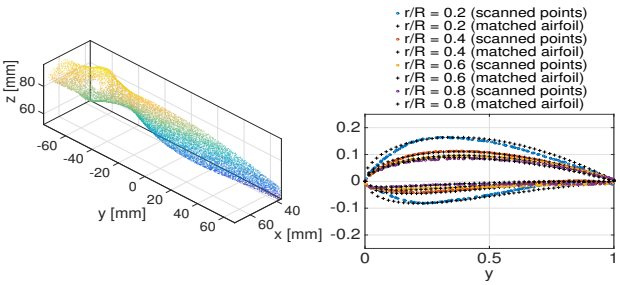

(a) 3D point cloud from scan (every 2000th point shown)

(b) Sectional airfoil sections (every 500th point shown)

Figure 1: 3D scan of an APC 10x7 Thin Electric propeller

Unstalled aerodynamic analysis

Aerodynamic data has been obtained for a wide range of Reynolds numbers, allowing accurate representation of the flow for the appropriate conditions. At any blade section, the aerodynamic coefficients are obtained as a function of both the local

angle of attack and the local Reynolds number. As an example, the variation of NACA 4412 airfoil data with Reynolds number is shown in Fig. 2, obtained using the computer program XFOIL.

Examining Figs 2a and 2b, XFOIL is seen to slightly overestimate the lift and drag for relatively high Reynolds numbers (250,000) relative to wind tunnel experimental data. This is consistent with the findings of [26]. At extremely low Reynolds numbers (20,000-30,000), XFOIL reproduces wind tunnel data relatively well, although the lift curve slope is overestimated, and the drag underestimated, consistent with the trends found for high Reynolds number data.

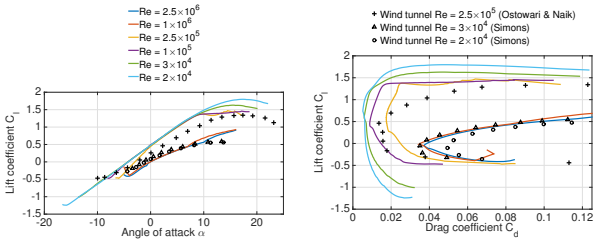

(a) Lift coefficient (b) Lift vs Drag coefficient

Figure 2: Aerodynamic data for the NACA4412 airfoil with wind tunnel data obtained from [13] and [27]

High angle of attack aerodynamic coefficients

The raw aerodynamic data generated using XFOIL has been extended using both flat plate theory and wind tunnel data. The flat plate method developed by Viterna and Corrigan [14] has been used, as well as wind tunnel testing of the NACA 4412 section by Ostowari and Naik [13].

The extension of aerodynamic data to post-stall angles of attack is shown in Fig. 3. When compared to wind tunnel tests [13], it is seen that at angles of attack greater than 45°, the Viterna-Corrigan [14] method reproduces lift coefficient fairly well. However the model makes no attempt to reproduce the initial drop and recovery of the lift coefficient seen in test data. Tangler and Ostowari [9] note that this omission produces no significant error. The post-stall drag coefficient produced by flat plate theory underpredicts drag by a significant amount. Meanwhile the most significant drawback of splining XFOIL polars to wind tunnel results is the unavailability of data points, particularly at negative angles of attack. It is especially notable in Fig. 3 where the data obtained by Ostowari and Naik [13] is only available to negative ten degrees.

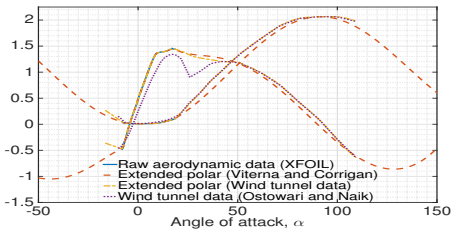

Figure 3: NACA 4412 airfoil data extended to high angles of attack (Re = 2.5×10^5, $AR = \infty$) and wind tunnel data [13]

Rotational effects

Rotational effects have been modelled using two different methods. A method based on the boundary layer equations was developed by Snel et al. [20]. This '3D correction method' models three dimensional flow effects due to rotation as an increase in the aerodynamic lift coefficient. Due to the extremely high chord to radius ratios at the hub of small propellers, the following modified version of the Snel 3D correction is used.

$$C_{l_{rot}} = C_{l_{non-rot}} + \frac{r}{R} \cdot \tanh\left(3.1 \cdot \left(\frac{\omega r}{V_b}\right)^2 \cdot \left(\frac{c}{r}\right)^2\right) \cdot (C_{l_{pot}} - C_{l_{non-rot}}) \quad (1)$$

The dependence on the relative radius term r/R ensures that the corrected lift coefficient remains realistic towards the blade root, while maintaining almost the full Snel 3D correction further along the blade. The Snel 3D correction is applied from the zero-lift angle to an angle of attack of 30 degrees. From this point, the correction is decreased linearly to zero at 50 degrees, where it rejoins the originally extended airfoil polar, following the implementation technique used by Lindenburg [16].

Meanwhile Corrigan and Schillings [21] developed a model whereby the stall of the airfoil is delayed to higher angles of attack and the maximum lift coefficient is increased. The delay of stall is expressed with a shift in the angle of attack for the non-rotating coefficients by the term $\Delta\alpha$. Additionally, the lift coefficient is increased according to the method used by Lindenburg [16]. The effects of the stall-delay model can be seen in Fig. 4.

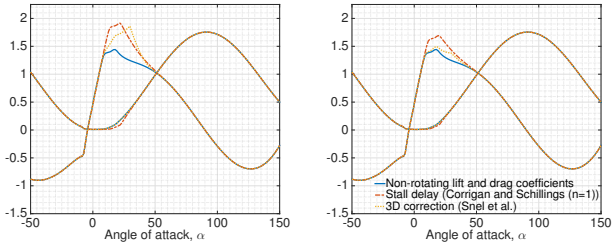

(a) $r/R = 0.45$ and $c/r = 0.4475$ (b) $r/R = 0.79$ and $c/r = 0.1473$

Figure 4: Rotating coefficients of a NACA4412 section propeller (Re = 2.5×10^5, $AR = 15$, V = 1m/s, RPM = 5000)

When implementing both methods, the drag values have been held constant, as there are conflicting views about the effects of rotation on drag [16]. The stall delay method does however shift the drag values to higher angles of attack, as seen in Fig. 4. Fig. 4 also shows that the stall delay method shows increased lift augmentation compared to the 3D correction developed by Snel et al. [20]. The effects of both methods decrease as the radius is increased (and the chord to radius ratio is reduced), though the 3D correction decreases in a far more pronounced fashion.

Towards the free end of a rotating propeller blade, the radial 'suction' due to centrifugal effects reduces significantly. However this radial flow from the inner part of the blade produces a reduction in the negative pressure on the upper surface of the airfoil compared to the non-rotating case. This reduces the lift coefficient in the tip region to below that of the non-rotating case. Following the model developed by Lindenburg [16], this reduction is applied from radial sections outboard of $0.8r/R$.

Results and Analysis

To validate the accuracy of developed extensions, two test cases were chosen. The APC Thin Electric 10x5 and 10x7 propellers were selected, and also have been wind tunnel tested [18, 29]. Both of the test propellers are model aircraft propellers, which routinely operate at low Reynolds numbers. The manufacturer

lists that each propeller uses a series of airfoils similar to Clark-Y and NACA4412 sections [30], however with the use of 3D scanning, the airfoil sections of each propeller were accurately identified at a number of radial sections, and are shown in Table 1. The geometry of each propeller is also extracted from the 3D scan, and gridded for analysis. The geometry of each propeller is shown and compared with geometry measurements from [18, 29] in Fig. 5.

Table 1: Propeller airfoil sections

	Propeller	
r/R	**APC 10x5**	**APC 10x7**
0.2	NACA5521	NACA4521
0.3	NACA4515	NACA5515
0.4	NACA5513	NACA5514
0.5	NACA5513	NACA5513
0.6	NACA4512	NACA4412
0.7	NACA4511	NACA4411
0.8	NACA4410	NACA4410
0.9	NACA4309	NACA4409
1.0	NACA4309	NACA4309

For each propeller, a number of simulations have been compared. A generic blade element momentum theory model is presented, using only data from a NACA 4412 section at a Reynolds number of 1×10^6. Full Reynolds number dependency and accurate airfoil sections have then been coupled with different combinations of high angle of attack and rotational effects methods. Finally the extended BEMT has been coupled with only a NACA4412 section while allowing Reynolds number to vary, and vice versa, to show the effect of each extension in turn.

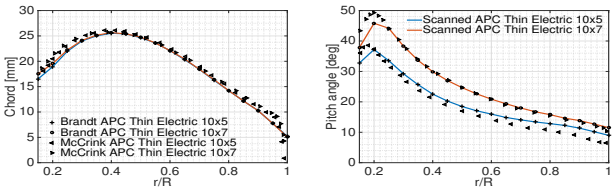

(a) Propeller chord (b) Propeller pitch

Figure 5: Geometry of APC Thin Electric propellers [30]

Through the simulation of both propellers, seen in Figs 6 and 7, there are a number of common trends. The generic BEMT model over-predicts thrust coefficient by a significant amount at all advance ratios, while also over-predicting power coefficient at higher advance ratios for both propellers. The generic model under predicts power at low advance ratios. These inaccuracies result in modelled efficiency curves that are significantly larger than those obtained from wind tunnel data.

Coupling the BEMT solution with the extended aerodynamic database significantly increases modelling accuracy. This is shown in modelling both thrust and power coefficients in Figs 6 and 7, with corresponding increases in the accuracy of efficiency modelling. Extension of aerodynamic polars to high angles of attack with wind tunnel data or the Viterna-Corrigan flat plate method produce fairly similar results, with the major differences seen at low advance ratios.

The two different methods used to model rotational effects do however cause significantly different modelled results at low advance ratios. The stall delay method [21] produces the most accurate prediction at low advance ratios, which can perhaps be attributed to the higher augmented lift when compared to the 3D correction [20], seen in Fig. 4. At low advance ratios, each extended method still over-predicts the power coefficient by a small margin, however the thrust modelling is highly accurate at all advance ratios.

When using the extended BEMT with just a NACA 4412 section, the results are less accurate than with full airfoil dependency, but not by as large an amount as might be expected. In the region where the most thrust and power is produced (around $0.7r/R$), each propeller has airfoils fairly similar to the NACA 4412 both in camber and thickness, thereby explaining the relatively small difference seen. However without prior knowledge of the airfoil sections that make up a propeller, estimation of an airfoil is often crude. In these situations, three dimensional scanning of the geometry offers invaluable insight into the aerodynamic polars required for analysis.

When average Reynolds numbers are used for each section combined with the extended BEMT, both thrust and power coefficients are overestimated throughout the advance ratio range, with increasing difference relative to wind tunnel data as the advance ratio is decreased. This can be attributed to the difference in aerodynamic coefficients when using averaged as compared to fully variable Reynolds numbers.

Conclusion

For generic blade element methods, aerodynamic analysis is usually limited to polars obtained for a single airfoil at a single Reynolds number, where data is provided for a limited angle of attack range. This leads to increasing inability to model propeller performance at low advance ratios.

In this paper, a number of extensions are made to the aerodynamic data upon which a blade element momentum model is based. Three dimensional scanning has been used to capture the airfoil sections that make up a propeller blade. Airfoil polars are then generated for each airfoil across a wide range of Reynolds numbers, allowing interpolation of aerodynamic data. Following this, aerodynamic data is extended to high angles of attack using both flat plate theory and wind tunnel data. Finally, the effects of rotation on the aerodynamic coefficients are captured using two different models, simulating the effects of radial flow. Significant improvements in modelling small propeller performance relative to a generic BEMT model have been shown. However at low advance ratios, power coefficient is still overestimated relative to wind tunnel results.

References

[1] Glassock, R., Design, modelling and measurement of hybrid powerplant for unmanned aerial vehicles (UAVs). Master's thesis, Queensland University of Technology, 2012.

[2] Verstraete, D., Gong, A., Lu, D. D.-C. and Palmer, J. L., Experimental investigation of the role of the battery in the AeroStack hybrid, fuel-cell-based propulsion system for small unmanned aircraft systems. *International Journal of Hydrogen Energy*, 40(3): 1598–1606, January 2015.

[3] Gong, A., Palmer, J. L., Brian, G., Harvey, J. R. and Verstraete, D., Performance of a hybrid, fuel-cell-based power system during simulated small unmanned aircraft missions. *International Journal of Hydrogen Energy*, 41(26):11418–11426, July 2016.

[4] Hendrick, P., Hallet, L. and Verstraete, D., Comparison of propulsion technologies for a HALE airship. *AIAA Aviation Technology, Integration and Operations Conference*, 1:527–534, 2007.

[5] Mair, W. A. and Birdsall, D. L., *Aircraft Performance*. Cambridge University Press, 1992.

[6] Gur, O. and Rosen, A., Propeller performance at low advance ratio. *Journal of Aircraft*, 42(2):435–441, March 2005.

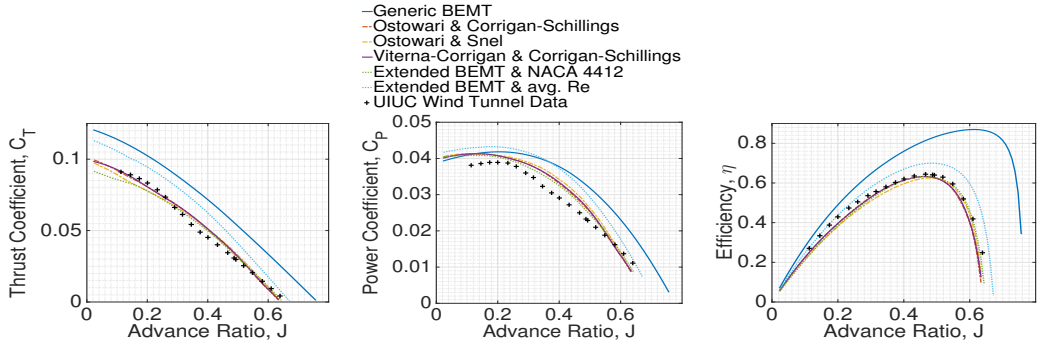

Figure 6: Analysis of APC Thin Electric 10x5 propeller at 5000rpm

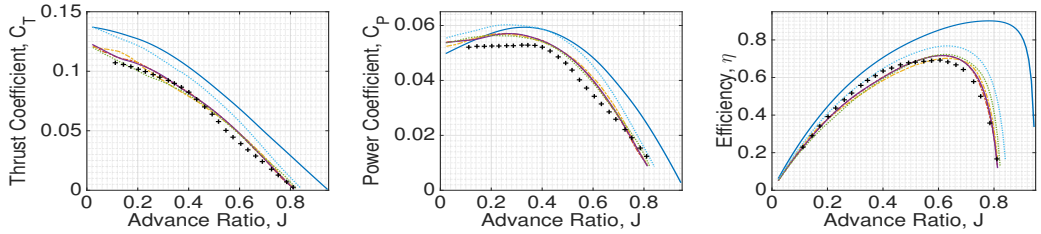

Figure 7: Analysis of APC Thin Electric 10x7 propeller at 5000rpm

[7] Morgado, J., Silvestre, M. Â. R and Páscoa, J. C., Validation of new formulations for propeller analysis. *Journal of Propulsion and Power*, 31(1), January 2015.

[8] Uhlig, D. V. and Selig, M. S., Post stall propeller behavior at low Reynolds numbers. *AIAA Aerospace Sciences Meeting and Exhibit*, January 2008.

[9] Tangler, J. L. and Ostowari, C., Horizontal axis wind turbine post stall airfoil characteristics synthesization. Technical report, United States Department of Energy, 1991.

[10] Montgomerie, B., Drag coefficient distribution on a wing at 90 degrees to the wind. Technical report, The Energy Research Centre of the Netherlands, 1996.

[11] Lindenburg, C., Aerodynamic airfoil coefficients at large angles of attack. *IEA Symposium on the Aerodynamics of Wind Turbines*, 2000.

[12] Critzos, C. C., Heyson, H. H. and Boswinkle Jr, R. W., Aerodynamic characteristics of NACA 0012 airfoil section at angles of attack from 0° to 180°. Technical report, National Advisory Committee for Aeronautics, January 1955.

[13] Ostowari, C. and Naik, D., Post-stall wind tunnel data for naca 44xx series airfoil sections. Technical report, Rockwell International Corp., January 1985.

[14] Viterna, L. A. and Corrigan, R. D., Fixed pitch rotor performance of large horizontal axis wind turbines. Technical report, NASA Lewis Research Center, 1982.

[15] Montgomerie, B., Methods for root effects, tip effects and extending the angle of attack range to plus/minus 180 degrees, with application to aerodynamics for blades on wind turbines and propellers. Swedish Defense Research Agency, June 2004.

[16] Lindenburg, C., Investigation into rotor blade aerodynamics. Technical report, National Renewable Energy Laboratory, July 2003.

[17] Ol, M. and Zeune, C., Analytical - experimental comparison for small electric unmanned air vehicle propellers. *AIAA Applied Aerodynamics Conference*, August 2008.

[18] McCrink, M. H. and Gregory, J. W., Blade element momentum modeling of low-Re small UAS electric propulsion systems. *AIAA Aviation*, 2015.

[19] Himmelskamp, H., Profile investigations on a rotating airscrew. *MAP Volkenrode, Reports and Translation*, (832), 1947.

[20] Snel, H., Houwink, R. and Bosschers, J., Sectional prediction of lift coefficients on rotating wind turbine blades in stall. Technical report, National Aerospace Laboratory (NLR), Netherlands, December 1994.

[21] Corrigan, J. J. and Schillings, J. J., Empirical model for stall delay due to rotation. *American Helicopter Society Aeromechanics Specialists Conference*, January 1994.

[22] Tangler, J. L. and Selig, M. S., An evaluation of an empirical model for stall delay due to rotation for HAWTS. *Windpower*, June 1997.

[23] Anemaat, W. A. J., Schuurman, M., Liu, W. and Karwas, A., Aerodynamic design, analysis and testing of propellers for small unmanned aerial vehicles. *Royal Aeronautical Society Applied Aerodynamics Conference*, 2016.

[24] Phillips, W. F., *Mechanics of Flight*. Wiley, 2nd edition, 2012.

[25] Drela, M., Xfoil: An analysis and design system for low reynolds number airfoils. *Low Reynolds Number Aerodynamics*, 1989.

[26] Maughmer, M. D. and Coder, J. G., Comparisons of theoretical methods for predicting airfoil aerodynamic characteristics. Technical report, The Pennsylvania State University, August 2010.

[27] Simons, M., *Model Aircraft Aerodynamics*. Special Interest Model Books, fourth edition, 1999.

[28] Xu, G. and Sankar, L. N., Application of a viscous flow methodology to the nrel phase-iv rotor. *ASME Wind Energy Symposium*, pages 83–93, 2002.

[29] Brandt, J. B., Small-scale propeller performance at low speeds. Master's thesis, University of Illinois at Urbana-Champaign, 2005.

[30] `https://www.apcprop.com/Articles.asp?ID=262airfoil` Last Accessed: July 2016